

# Structural shape reconstruction of non-linear systems via Variational Autoencoders

Roberta Cumbo<sup>1,\*</sup>, Roberto Morelli<sup>2</sup>, Abhishek Kumar<sup>3</sup> and Alessandro Nicolosi<sup>4</sup>

<sup>1</sup>Lab of Materials Technologies, Leonardo Labs, Via Tiburtina Km. 12.400, Roma, 00156, Italy

<sup>2</sup>Lab of Artificial Intelligence, Leonardo Labs, Via Pieragostini 80, Genova, 16149, Italy

<sup>3</sup>Lab of Materials Technologies, Leonardo Labs, Via dell'Aeronautica, Pomigliano d'Arco, 80038, Italy

<sup>4</sup>Lab of Artificial Intelligence, Leonardo Labs, Via Tiburtina Km. 12.400, Roma, 00156, Italy

## Abstract

The application of Variational Auto-Encoders (VAE) for full-field displacement reconstruction of a general non-linear system is shown in this contribution to the framework of Structural Health Monitoring (SHM). The presented approach aims to combine sensor data with a Finite Element representation of the structure, addressing the problem of Model Order Reduction by using a Proper Orthogonal Decomposition approach. Physics knowledge of the system is embedded into the VAE model which is trained to correctly reproduce non-linearities in the system. The model is evaluated both from the reconstruction and prediction point of view in order to define possible limitation of the proposed approach as a tool for SHM.

## Keywords

Structural Health Monitoring, Reduced Order Modelling, Variational Auto-Encoders, Finite Element Analysis

## 1. Introduction

The on-board integration of Structural Health Monitoring (SHM) systems can improve the safety and reliability of aerospace and automotive structures during operational life by preventing structural components from catastrophic failure scenarios and identifying possible damages sooner than common manual inspection. The role of online parameters and load identification, together with stress field distribution, is nonetheless of paramount importance. With the advances in the development of predictive algorithms in the field of Artificial Intelligence (AI), physics-informed solutions have attracted great attention in the field of SHM, by combining sensor data with the numerical model of the monitored structure. The choice of installed sensors depends on the application. For example, Digital Image Correlation (DIC) and Fiber Bragg Grating (FBG) systems can be respectively employed for shape reconstruction and critical stress paths identification. The challenge in SHM is to optimally define the map of such sensors which is able to retrieve not-measured sensor data. Inverse identification from a reduced set of measured data to full-field response is pos-

sible starting from the knowledge of a numerical model which is a digital representation of the physical system. In the field of structural mechanics, Finite Element Models (FEMs) [1] are usually adopted to simulate the real structure. Reduced Order Modelling (ROM) [2, 3] algorithms are employed when complex FEM are involved to reduce computational costs. Several methodologies have been presented in the literature to address the system identification task on dynamic structures by embedding ROM models. One of the most used approaches is the Kalman Filter (KF), which has been extensively investigated for the estimation of loads, parameters, and full-field response [4, 5, 6]. The main advantage of KF is that the baseline FE model needs to capture the main dynamics of the system but high-correlated models are not needed. In the last few years, AI-based techniques have become competitive solutions. In particular, the Auto-Encoders (AEs) and the variational counterpart, i.e. Variational Auto-Encoders (VAE) [7] have been widely used in literature to approach model order reduction problems [8, 9, 10, 11]. The structure of the AEs defined by an encoder, a latent space with a reduced order and a decoder, has several similarities with the principles of ROM. The formulation in the latent space is user-defined. If there is no knowledge of the dynamical system, the latent space is fully defined as a black-box model. In other hand, if there is perfect knowledge of the model, the latent space will be defined as a white-box model identified by the ROM of our system. In a real case scenario, black or white box modeling is never the case because the main dynamic of the system is assumed to be known from design and validation of the investigated structure. The customized setting of the latent space in AEs or VAEs

*Ital-IA 2023: 3rd National Conference on Artificial Intelligence, organized by CINI, May 29–31, 2023, Pisa, Italy*

\*Corresponding author.

✉ roberta.cumbo.ext@leonardo.com (R. Cumbo);

roberto.morelli.ext@leonardo.com (R. Morelli);

abhishek.kumar@leonardo.com (A. Kumar);

alessandro.nicolosi@leonardo.com (A. Nicolosi)

📞 0000-0003-1204-4492 (R. Cumbo); 0000-0001-5090-9026

(R. Morelli); 0000-0001-9299-6228 (A. Kumar); 0009-0007-5071-5687

(A. Nicolosi)

© 2022 Copyright for this paper by its authors. Use permitted under Creative Commons License

Attribution 4.0 International (CC BY 4.0).

CEUR Workshop Proceedings (CEUR-WS.org)



gives an advantage over KF methodologies, allowing for the estimation of missing physics in the FE model.

In this contribution, an application of VAE to full-field displacement estimation is presented by implementing a sliding time-windowing approach. The use-case is a non-linear cantilever beam and a Proper Orthogonal Decomposition (POD) [12] reduction basis is adopted. The article is structured as follows: the state-space formulation of a FE model, the POD approach, and VAE are described in Sec. 2; following, the use-case and the results obtained through VAE are shown in Sec. 3.

## 2. Methodology

### 2.1. State-space formulation of a structural dynamic system

The governing equation of motion of a dynamical system described by the mass matrix  $\mathbf{M}$ , the stiffness matrix  $\mathbf{K}$  and the damping matrix  $\mathbf{D}$  is:

$$\mathbf{M}\ddot{\mathbf{x}} + \mathbf{K}\mathbf{x} + \mathbf{D}\dot{\mathbf{x}} + \mathbf{f}(\mathbf{x}) = \mathbf{B}\mathbf{u} \quad (1)$$

Where  $\mathbf{x} \in \mathbb{R}^{n_d}$ ,  $\dot{\mathbf{x}} \in \mathbb{R}^{n_d}$ ,  $\ddot{\mathbf{x}} \in \mathbb{R}^{n_d}$  are respectively the Degrees of Freedom (DoFs) of the system with size  $n_d$  and their first and second derivative with respect to time. The time dependence of these variables has been omitted for simplicity.  $\mathbf{B}$  and  $\mathbf{f}(\mathbf{x})$  are respectively the Boolean matrix that distributes the inputs vector  $\mathbf{u}$  over the DoFs of the system and a general nonlinear term.

By assuming  $\mathbf{f}(\mathbf{x}) = 0$ , Eq. 1 can be re-written in a state-space formulation as follows:

$$\begin{cases} \dot{\mathbf{x}}_s = \mathbf{A}\mathbf{x}_s + \mathbf{B}_s\mathbf{u} \\ \mathbf{y} = \mathbf{C}\mathbf{x}_s + \mathbf{D}_s\mathbf{u} \end{cases} \quad (2)$$

where  $\mathbf{x}_s = [\mathbf{x}, \dot{\mathbf{x}}]^T$  is the state vector,  $\mathbf{A}$  and  $\mathbf{B}_s$  are obtained from Eq.1. The second equation of the system is the measurement equations, where  $\mathbf{y} \in \mathbb{R}^{n_m}$  is the measurements vector with size  $n_m$  and  $\mathbf{C}$ ,  $\mathbf{D}_s$  are matrix depending on the measurements' type.

### 2.2. Reduction basis: Proper Orthogonal Decomposition approach for non-linear systems

ROM can be required when the number of DoFs  $n_d$  of a FEM is too large and, consequently, the computational cost is too high. The projection of the Full Order Model (FOM) to the ROM is defined by the following approximation:

$$\dot{\mathbf{x}} \cong \Phi\dot{\mathbf{q}} \quad (3)$$

where  $\Phi \in \mathbb{R}^{n_d \times n_r}$  is the reduction basis mapping  $n_d$  DoFs to  $n_r$  reduced DoFs  $\mathbf{q} \in \mathbb{R}^{n_r}$ .

When non-linear systems are involved, standard ROM approaches as Guyan [2] or Craig-Bampton [3] can not be applied. The Proper Orthogonal Decomposition (POD) [12] method is one of the most used approaches for non-linear dynamics. POD identifies an optimal subspace based on a set of snapshots, i.e. time series data, of the system solution space. In other words, the main principle of the POD is in the selection of the meaningful shapes or modes of the solution provided by snapshots of e.g. displacements or velocities through a Singular Value Decomposition (SVD). Given the matrix of snapshots  $\mathbf{x} \in \mathbb{R}^{n_d \times n_t}$ , with  $n_t =$  number of time samples ( $n_t \geq n_d$ ), the SVD gives:

$$\mathbf{x} = \mathbf{U}\mathbf{S}\mathbf{V} \quad (4)$$

with  $\mathbf{U} \in \mathbb{R}^{n_d \times n_d}$  and  $\mathbf{V} \in \mathbb{R}^{n_t \times n_t}$  as left and right singular vectors respectively and  $\mathbf{S} \in \mathbb{R}^{n_d \times n_d}$  as diagonal matrix containing the singular values on the main diagonal. The POD forms the reduction basis by selecting the first  $r$ -left singular values ( $r < n_d$ ) from the matrix  $\mathbf{U}$ , such that the following minimization problem is reached:

$$\min \|\mathbf{x} - \mathbf{q}\|_2 \quad (5)$$

The number of selected values depends on the threshold selected.

The POD has the disadvantage of requiring the snapshots matrix, which needs to be computed offline using FOM simulations. However, as a main advantage, the POD reduction basis provides a higher accuracy for non-linear and parametric models, as these characteristics are present in the solution space and captured via the snapshots. Furthermore, the selection of the meaningful singular values also has a physical interpretation on the solution. A good explanation can be found in [13]. If a parametric model is considered, other techniques need to be employed in order to have the POD basis working for all the parameters samples, i.e. global reduction basis. The most common ways are by interpolating or concatenating the POD basis obtained for each sample. When the number of samples is limited, the concatenation approach is the easiest one. Given a set of  $p$  concatenated basis, the SVD is recomputed in order to remove possible linear dependencies between all the subspaces, as follows:

$$\text{SVD} \left( [U_1 \ U_2 \ U_3 \ \dots \ U_p] \right) \quad (6)$$

Given thus as global reduction basis of the mechanical non-linear system, Eq. 2 projected in the reduced space can be re-written as:

$$\begin{cases} \dot{\mathbf{z}} = \mathbf{A}_r\mathbf{z} + \mathbf{B}_r\mathbf{u} \\ \mathbf{y} = \mathbf{C}_r\mathbf{z} + \mathbf{D}_r\mathbf{u} \end{cases} \quad (7)$$

where  $\dot{\mathbf{z}} = [\dot{\mathbf{q}}, \mathbf{q}]^T$  is the reduced state vector and all the matrices are in a reduced form.

**Table 1**

Model architecture. List of modules with number of layer, neurons and the total number of parameters.

Architecture	layers	neurons	parameters
MLP	2	[16, 8]	446
LSTM	1	64	19598
Ode Model model	3	[128, 64, 32]	15294
			35338

### 2.3. Variational Auto-Encoder for Model Order Reduction

In this section, the principles of VAE addressing ROM are described and schematically shown in Fig. 1. The formulation used in this article is the same presented in [8] and regard the extension of the variational autoencoder model to their dynamic version. Specifically, by including a recurrent neural network into the standard fully-connected layer, such architecture can process time series data. So, starting from a subset of sensor data, the following module are used to process a multidimensional time-series data:

- Encoder: data-driven, i.e. no physics of the system considered at this stage. It is composed by two sub-networks: a Multilayer Perceptron (MLP) and Long Short Term Memory (LSTM) returning respectively distributions of initial conditions at position  $\mathbf{q}_0 \in \mathbb{R}^{n_r}$  and velocity  $\dot{\mathbf{q}}_0 \in \mathbb{R}^{n_r}$  level of the reduced model. The concatenation of  $\mathbf{q}_0$  and  $\dot{\mathbf{q}}_0$  forms the initial state vector  $\mathbf{z}_0 \in \mathbb{R}^{2n_r}$ .
- Latent Model: physics-informed, modelled as residual models, i.e.  $\mathbf{f}_{\text{baseline}}(\mathbf{z}) + \mathbf{f}_{\text{NN}}(\mathbf{z})$ . From Eq. 7:  $\mathbf{f}_{\text{baseline}}(\mathbf{z}) = \mathbf{A}_r \mathbf{z}$ . The non-linear term is instead added  $\mathbf{f}_{\text{NN}}(\mathbf{z})$  to compensate for model truncation and for non-linearities (if any) as in Eq. 1. In the latent space stage, the integration of the state space model over time is performed.
- Decoder: it represents the reduction basis  $\Phi$  and can be trainable or not-trainable, e.g. pre-computed via POD. It allows to retrieve FOM data from the latent space.

In table 1 is reported some details about the architecture.

The Evidence Lower Bound (ELBO) loss is commonly used with VAE as objective function to be minimized. This loss can be formulated as follows:

$$L_{\text{ELBO}} = -\text{KL}(q(z|x)||p(z)) + E_{q(z|x)} [\log p(x|z)] \quad (8)$$

where  $\text{KL}(q(z|x)||p(z))$  is the Kullback-Leibler (KL) divergence between the learned posterior distribution and the prior distribution over the latent variables. The first term encourages the learned posterior to be close to the

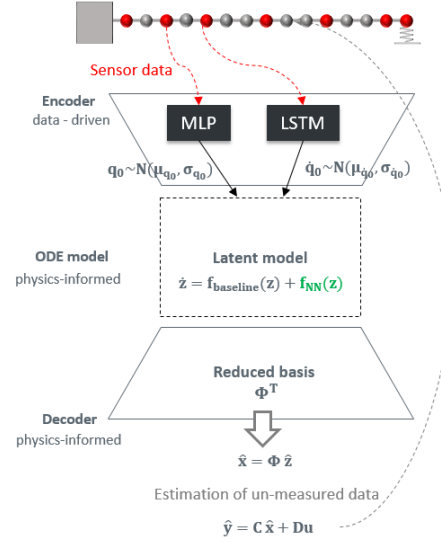


**Figure 1:** Scheme of VAE applied to reduced numerical model starting from the knowledge of sensor data.

prior, while the second term encourages the VAE to reconstruct the observed data accurately. Minimizing the ELBO loss in a VAE corresponds to find the optimal trade-off between reconstruction accuracy and regularization of the learned posterior distribution. Moreover, to get a better reconstruction quality, the posterior distribution can be explicitly derived in place of the standard mean squared loss. In this work, a normal distribution is used:

$$f(x) = \frac{1}{\sigma\sqrt{2\pi}} \exp\left(-\frac{(x - \hat{x})^2}{2\sigma^2}\right) \quad (9)$$

where  $x$  is a time step of the input sequence,  $\hat{x}$  is the model output,  $\sigma$  is the standard deviation. This latter term is a constant equal to  $3e - 2$

### 3. Non-linear cantilever beam use-case

The object of the current study is a cantilever Euler-Bernoulli beam, with an end non-linear grounded spring (Fig. 2). This benchmark has been presented and studied in several contributions [14, 15, 16]. The model here is characterized by the following parameters: density  $\rho = 2700 \text{ kg/m}^3$ , cross-sectional inertia  $I = 4.3e^{-9} \text{ m}^4$ , sectional area  $A = 3.23e^{-4} \text{ m}^2$ , stiffness parameter  $k_n = \frac{3EI}{L^3} = 3e^3 \text{ N/m}$ , first natural frequency  $\omega = 1 \text{ rad/s}$ ,  $\alpha^4 = \omega^2 \frac{\rho AL^4}{EI}$ , proportional damping factor  $\zeta = 1e^{-4}$ . The model has been discretized via 2D FE analysis with  $N_e = 15$  beam elements. The DoFs of the system are the

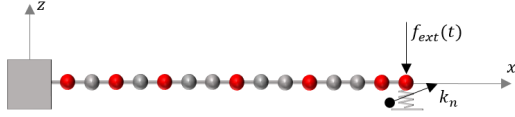


**Figure 2:** Schematic representation of the FE model of a clamp-free beam with a grounded spring.

vertical displacement in  $z$  direction and rotation along  $y$ -axis, for a total of  $n_d = 2N_e$ . The system has been simulated via Euler implicit integrator in a time window of  $T = 100s$ . The parameter  $k_n$ , associated to the non-linear spring, is sampled in order to create the dataset for different values of non-linearities. The values of  $k_n$  range in  $[1e^{-9}, 9e^{-9}]N/m$  and 5 uniformly distributed samples are selected. The beam is loaded at the tip with a sinusoidal force along  $z$ -direction:

$$f_{ext}(t) = 12 \sin 6t + 9 \sin \pi \frac{t - 2e^3}{0.05} \quad (10)$$

Differently from the contribution in [8], the global reduction basis  $\Phi$  is computed through SVD by concatenating local reduction basis as in Eq. 6. Each local basis is obtained via POD which is applied to the snapshots of each solution in the range of  $k_n$  parameter. The singular values after concatenation and the first three mode shapes are shown in Fig. 3 and Fig. 4. The mode shapes show differences with standard normal modes of a cantilever beam because of the effect of the non-linearities. A total of 7 modes, i.e.  $n_r = 7$  is selected from SVD analysis. This number results to be the optimal one by comparing reference with reconstructed time data. This reduction basis allows the model to capture all the non-linearities presented in the simulated dataset. In [? ], the decoder is defined by the reduction basis coming from eigenanalysis of the linear model. That approach can however lead the model to be projected in a wrong reduction basis and thus to a wrong reconstruction. The comparison between the two approaches is out of the scope of this article. Anyway, the choice of using a POD is the most suitable for the analyzed system, according to theory in [12].

### 3.1. Displacement field estimation through VAE

The scope of this work is to train a VAE to estimate the dynamical behavior of  $n_d = 30$  DoFs of the cantilever beam starting from a subset of DoFs. These limited number of measurements has been defined in order to guarantee the observability of the system and are the 7 measures marked in red in Fig. 2. To train such architecture on the data simulated following the process described in

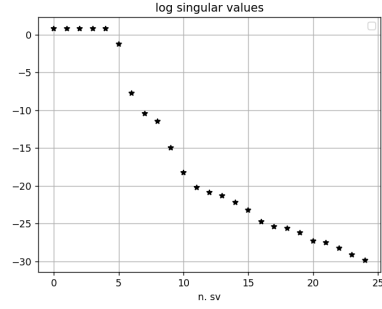


**Figure 3:** Singular values of the concatenated basis.

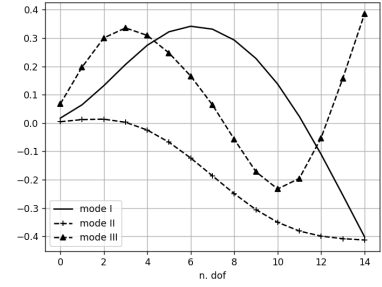


**Figure 4:** First three mode shapes of the POD basis.

section 3, a windowing approach is defined. Specifically, the temporal sequences of each DoF are split into several temporal windows with a length defined a-priori. In this way, the dataset is augmented and the windowing allows the encoder to learn the model non-linearities and the initial conditions of the latent model starting from the time-series of a subset of observations.

Among the 5 simulated samples, 4 of these are used for the training. Each sample describes the cantilever beam behaviour in a range of 10000 time steps. The size of the train set is thus equal to 40000 time steps. The windowing is performed with a fixed size of 200 time steps. The sample generated with a value of  $k_n$  in the middle of the specified range of parameters identifies the validation set. A scheduler is also implemented such that if the validation loss doesn't improve after 5 epochs, the learning rate decreases to the 80% of its previous value. A batch size of 32 is used and the model reaches its optimal state after nearly 25 epochs. The reason why the loss converges after few epochs is justified by the high number of data that the model processes for each epoch. An early stopping of 20 epochs is used. The trend of the train and validation losses normalized with respect to the value of the training loss at the first epoch is shown in Fig. 5. The validation loss is always lower than the training loss because the validation set has been defined in the middle of the sampling parameter range. However,

a more challenging validation set should be also tested in order to quantify the overall performances of the model.

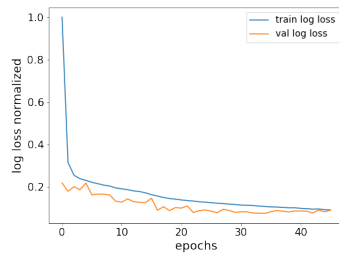


**Figure 5:** Train and validation normalized loss trend epoch by epoch.

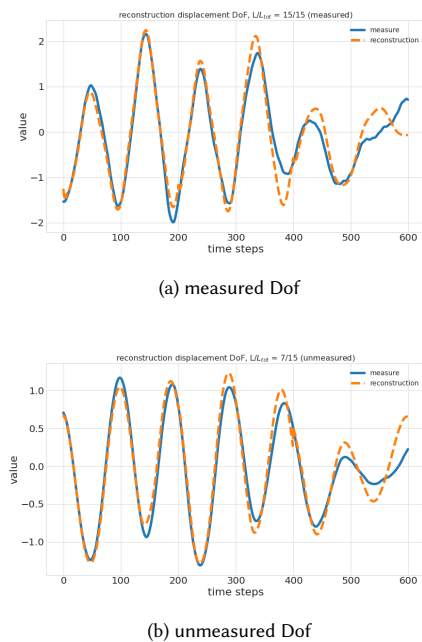
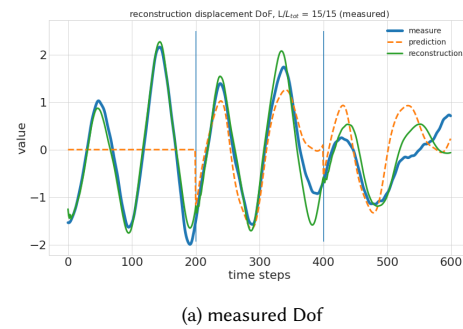
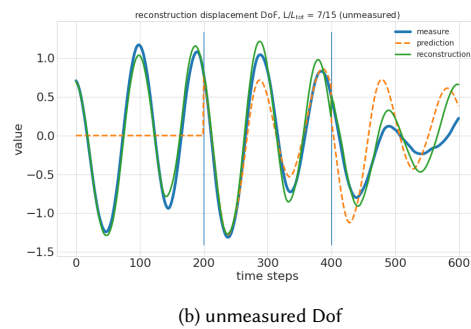


**Figure 6:** Time history reconstruction of an un-measured and a measured DoF.

The results are reported for the sequences belonging to the validation set. The model is trained to reconstruct all the DoFs of the system starting from a subset. In Fig. 6, are reported the results concerning both an un-measured and one measured DoFs. From these plots it is possible to observe that the model is able to catch the dynamics of the signals. These DoFs have been chosen without loss of generality on the overall performances. In Fig. 3.1 are reported the result for the prediction task. In this latter scenario, the model receives in input a sequence of 200 time steps and predicts also the next 200 time steps. The



(a) measured DoF



(b) unmeasured DoF

**Figure 7:** Model prediction in a time horizon of 600 steps: the green line refers to the reconstruction of the sequences while the next one shows the prediction of each window for the next 200 time steps.

results are shown in Fig. 3.1 and Fig. 3.1 over a greater time horizon. For each window, the prediction coming from the previous window and the actual reconstruction are compared. This comparison is shown starting from time step 200, i.e. second window. From the reported results, the prediction is in some cases accurate. However, we observe that this estimation depends drastically from the input sequence and generally does not produce reliable estimation. A more accurate training could perhaps return more reliable prediction.

## 4. Conclusions

The application of the Variational Auto-Encoder to non-linear dynamics is shown in this article. A non-linear cantilever beam is investigated by simulating the Finite Element model with different values of non-linear parameters. The simulated dataset allows to form the reduction basis by performing a snapshots-based Proper Orthogonal Decomposition. This step leads to a pre-defined decoder in the VAE architecture by reducing the number of total trainable parameters. However, a trainable decoder could give some advantages e.g. more adapt-



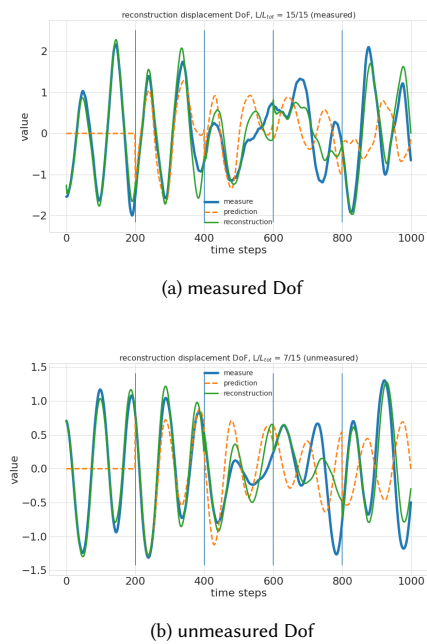


**Figure 8:** Model prediction in a time horizon of 1000 steps: the green line refers to the reconstruction of the sequences while the yellow one shows the prediction for the next 200 time steps.

able reduction basis with respect to training data. The latent model described as residual grey-box model of the system dynamics allows also for the identification of all the contributions that have not been implemented in the baseline model as e.g. external forces, parameters, and non-linearities. In a real test case, the available dataset is normally not enough for a deep learning application and thus the windowing approach has been tested in order to perform data augmentation. The analysis shown in this article led to accurate results in the estimation of un-measured data, starting from the knowledge of a subset of measurements. The structure of the presented approach with time windowing and a pre-trained model can be used for online structural monitoring applications.

## References

- [1] O. Zienkiewicz, R. Taylor, *The Finite Element Method*, Butterworth Heinemann, Oxford, 2000.
- [2] R. J. Guyan, Reduction of stiffness and mass matrices, *AIAA journal* 3 (1965) 380–380.
- [3] R. R. Craig Jr, M. C. Bampton, Coupling of substructures for dynamic analyses, *AIAA journal* 6 (1968) 1313–1319.
- [4] R. Cumbo, T. Tamarozzi, K. Janssens, W. Desmet, Kalman-based load identification and full-field estimation analysis on industrial test case., *Mechanical Systems and Signal Processing* 117 (2019) 771–785.
- [5] E. Risaliti, T. Tamarozzi, M. Vermaut, B. Cornelis, W. Desmet, Multibody model based estimation of multiple loads and strain field on a vehicle suspension system, *Mechanical Systems and Signal Processing* 123 (2019) 1–25.
- [6] C. E. Capalbo, D. De Gregoriis, T. Tamarozzi, H. Dervriendt, F. Naets, G. Carbone, D. Mundo, Parameter, input and state estimation for linear structural dynamics using parametric model order reduction and augmented kalman filtering, *Mechanical Systems and Signal Processing* 185 (2023) 109799.
- [7] D. P. Kingma, M. Welling, Auto-encoding variational bayes, *arXiv preprint arXiv:1312.6114* (2013).
- [8] Z. Lai, W. Liu, X. Jian, K. Bacsá, L. Sun, E. Chatzi, Neural modal ordinary differential equations: Integrating physics-based modeling with neural ordinary differential equations for modeling high-dimensional monitored structures, *Data-Centric Engineering* 3 (2022) e34.
- [9] T. Simpson, N. Dervilis, E. Chatzi, Machine learning approach to model order reduction of nonlinear systems via autoencoder and lstm networks, *Journal of Engineering Mechanics* 147 (2021) 04021061.
- [10] M. Banihashemi, F. and Weber, W. Lang, Model order reduction of building energy simulation models using a convolutional neural network autoencoder, *Building and Environment* 207 (2022) 108498.
- [11] M. Mrosek, C. Othmer, R. Radespiel, Variational autoencoders for model order reduction in vehicle aerodynamics, *AIAA Aviation 2021 Forum* (2021) 3049.
- [12] P. Benner, S. Gugercin, K. Willcox, A survey of projection-based model reduction methods for parametric dynamical systems, *SIAM review* 57 (2015) 483–531.
- [13] J. Weiss, A tutorial on the proper orthogonal decomposition, *AIAA Aviation 2019 Forum* (2019) 3333.
- [14] M. Gürgöze, On the eigenfrequencies of a cantilever beam with attached tip mass and a spring-mass system, *Journal of Sound and Vibration* 190 (1996) 149–162.
- [15] M. W. Sracic, M. S. Allen, Numerical continuation of periodic orbits for harmonically forced nonlinear systems, *Civil Engineering Topics* 4 (2011) 51–69.
- [16] M. S. Allen, M. W. Sracic, System identification of dynamic systems with cubic nonlinearities using linear time-periodic approximations, *International Design Engineering Technical Conferences and Computers and Information in Engineering Conference* 49019 (2009) 731–741.